NUWC-NPT Technical Report 11,132
18 June 1999

# Efficient Discrete Fourier Representation of Pulse Responses

**Thomas A. Wettergren**
Torpedo Systems Technology Department




**Naval Undersea Warfare Center Division**
**Newport, Rhode Island**

## PREFACE

This work was sponsored by the Office of Naval Research under the Undersea Weaponry Guidance and Control (G&C) Project, Task 2, Advanced G&C Technology, and Task 3, Simulation and Test; principal investigator Daniel J. O'Neill (Code 8212). The ONR program manager is Khine Latt (Code 333).

The technical reviewer for this report was Carlos Godoy (Code 8213).

**Reviewed and Approved: 18 June 1999**

**James C. S. Meng**
**Head, Torpedo Systems Technology Department**

# REPORT DOCUMENTATION PAGE

*Form Approved*
*OMB No. 0704-0188*



| 1. AGENCY USE ONLY (Leave Blank) | 2. REPORT DATE | 3. REPORT TYPE AND DATES COVERED |
|---|---|---|
| | 18 June 1999 | Final |

4. TITLE AND SUBTITLE

EFFICIENT DISCRETE FOURIER REPRESENTATION OF PULSE RESPONSES

5. FUNDING NUMBERS

PR F821219
PR W821219

6. AUTHOR(S)

Thomas A. Wettergren

7. PERFORMING ORGANIZATION NAME(S) AND ADDRESS(ES)

Naval Undersea Warfare Center Division
1176 Howell Street
Newport, RI 02841-1708

8. PERFORMING ORGANIZATION REPORT NUMBER

TR 11,132

9. SPONSORING/MONITORING AGENCY NAME(S) AND ADDRESS(ES)

Office of Naval Research
800 North Quincy Street
Arlington, VA 22217-5160

10. SPONSORING/MONITORING AGENCY REPORT NUMBER

11. SUPPLEMENTARY NOTES

12a. DISTRIBUTION/AVAILABILITY STATEMENT

Approved for public release; distribution is unlimited.

12b. DISTRIBUTION CODE

13. ABSTRACT (Maximum 200 words)

The problem of modeling the transient response of a linear system to an incident pulse (finite time series) is examined. In mathematical modeling, this problem is solved through the convolution of a time domain pulse with a model-generated transfer function (spectral Green's function) of the linear system under consideration. This report is concerned with a particular class of linear systems, i.e., those that are separable into a superposition of multiple linear subsystems. Such problems arise often in high-frequency acoustics applications, where ray theory is applied and the linear acoustic system is represented as a superposition of many acoustic rays of energy.

14. SUBJECT TERMS

Acoustic models
Signal processing
Underwater acoustics

15. NUMBER OF PAGES
26

16. PRICE CODE

| 17. SECURITY CLASSIFICATION OF REPORT | 18. SECURITY CLASSIFICATION OF THIS PAGE | 19. SECURITY CLASSIFICATION OF ABSTRACT | 20. LIMITATION OF ABSTRACT |
|---|---|---|---|
| Unclassified | Unclassified | Unclassified | SAR |

## TABLE OF CONTENTS



## LIST OF ILLUSTRATIONS

# EFFICIENT DISCRETE FOURIER REPRESENTATION OF PULSE RESPONSES

## INTRODUCTION

The problem considered in this report is the modeling of the transient response of a linear system to an incident pulse (finite time series). In mathematical modeling, this problem is solved[1] through the convolution of a time domain pulse with a model-generated transfer function (spectral Green's function) of the linear system under consideration. This report is concerned with a particular class of linear systems, i.e., those that are separable into a superposition of multiple linear subsystems. Such problems arise often in high-frequency acoustics applications, where ray theory is applied and the linear acoustic system is represented as a superposition of many acoustic rays of energy.

The convolution of a time domain pulse with a linear system is a well-known problem in linear systems theory[2,3] that arises often in areas such as signal processing and control systems. The techniques used are based on a Fourier representation of the system and the incident pulse in the frequency domain. Simple convolution provides the system output in the time domain. The superposition principle allows addition of subsystem responses in either the time or frequency domains, the latter of which is much more straightforward yet computationally inefficient. By examining the practical nuances of the time domain approach, a computationally efficient method of superposition of subsystems can be developed.

In this report, a numerically efficient technique is presented for the computational problem of mathematically modeling the convolution of a transient pulse with a set of subsystem transfer functions. Both the theoretical and practical limitations of this technique, as well as the standard approach, are presented. The results of the technique are shown in the context of two problems of Navy importance: acoustic scattering from a multiple-highlight structure and acoustic propagation modeling using eigenray bundles. Results are presented in the context of both computational efficiency as well as numerical accuracy. The technique is developed in a general framework such that its extension to other applications is straightforward. The report concludes with general guidance on the utility of the technique in applications.

## TRANSIENT PULSE RESPONSE MODELING FOR A SINGLE SYSTEM

The modeling of steady-state phenomena is a common practice in many areas of science and engineering. Often, these are the only models that can be analytically and/or numerically solved in an efficient manner; therefore, many engineering decisions are made based on steady-state models even when the process under consideration is not steady-state. However, in the case of linear input/output systems, the steady-state response can be used to determine transient behavior. In this section, the standard approach for modeling transient responses using steady-state models is developed and discussed.

The process that is being modeled is assumed to have a single (scalar) input and single (scalar) output. This is an assumption that is made for notational convenience only, as the multi-input, multi-output case is a simple extension with no theoretical differences. Furthermore, assume that the process being modeled is representable by an impulse response function (or Green's function) given by $h(t)$. Using the theory of linear systems,[1,2] the response $y(t)$ of the system to a pulse $u(t)$ is given by the convolution

$$y(t) = \int_{-\infty}^{+\infty} h(\tau)u(t-\tau)d\tau. \tag{1}$$

The only assumptions required in equation (1) are that the system is a linear time-invariant system and the input pulse $u(t)$ is a real excitation. Note that if the system is causal, then $h(t) = 0$ for all $t < 0$; thus, in that case the integral may be taken from 0 to $+\infty$. The expression in equation (1) can be placed in the frequency domain by Fourier transforming both sides to yield

$$Y(\omega) = H(\omega)U(\omega), \tag{2}$$

which is a standard result from elementary linear systems theory. In expression (2), the term $Y(\omega)$ is used to represent the Fourier transform of $y(t)$, and similarly for $H(\omega)$ and $U(\omega)$. In this notation, $H(\omega)$ is referred to as the transfer function of the system.

If the system under examination is subjected to a unity amplitude steady-state input of frequency $\omega_0$, then the resulting output is given by (upon inspection of equation (2))

$$Y(\omega_0) = H(\omega_0). \tag{3}$$

Thus, the transfer function $H(\omega_0)$ at any frequency $\omega_0$ can be found as the response of the system to a steady-state input of frequency $\omega_0$. This provides a convenient means of numerically determining a transfer function by running a steady-state model at any required frequency. Since many mathematical models of complex systems are derived in a steady-state manner, this is usually a straightforward extension of an existing model. It

should be noted, however, that this technique only provides samples of the transfer function at a discrete set of frequencies, rather than the continuous function $H(\omega)$. Furthermore, the transfer function is, in general, a complex quantity, and thus any model must accurately produce both the magnitude and phase of the steady-state output for application as a sampled transfer function. Many existing steady-state models are only validated for magnitude, and phase validation over the frequency range of application is a necessity for transient response modeling. Thus, additional validation of the steady-state model is often required prior to its use in transient response modeling.

The mathematical modeling problem of interest is to convolve a given (non-steady-state) pulse with a system defined by an impulse response function. For the purposes of this report, it will be assumed that the system in question has been adequately modeled for steady-state response and that a numerical model of that process exists. It is further assumed that the steady-state model has been validated for both magnitude and phase over the frequency range of interest. Some examples of available models in acoustics are finite-element models of structural acoustic response, environmental propagation models for a fixed source/receiver pair, and acoustic scattering models for a single highlight.

Let $h(t)$ denote the system's impulse response function (Green's function). Accordingly, let $H(\omega_j)$ denote the transfer function of the system (steady-state model output) at a frequency $\omega_j$, which is a sampling of the Fourier transform of $h(t)$ at a specific frequency. Let $p(t)$ represent a real input pulse. It is assumed that $p(t)$ is non-zero only over a finite interval of time from $t = t_0$ to $t = t_1$. From expressions (1) and (2), it is easily seen that the system response is given by

$$\begin{aligned} y(t) &= F^{-1}\{Y(\omega)\} \\ &= F^{-1}\{H(\omega)P(\omega)\} \\ &= F^{-1}\{H(\omega)F\{p(t)\}\}, \end{aligned} \tag{4}$$

where $F\{\}$ represents the Fourier transform and $F^{-1}\{\}$ represents the inverse Fourier transform. Using a Fourier transform pair of the form

$$G(\omega) = \int_{-\infty}^{+\infty} g(t)e^{-i\omega t}\,dt, \tag{5a}$$

and

$$g(t) = \frac{1}{2\pi}\int_{-\infty}^{+\infty} G(\omega)e^{i\omega t}\,d\omega, \tag{5b}$$

it can be shown that equation (4) is equivalent to

$$y(t) = \left(\frac{1}{2\pi}\right)\iint H(\omega)p(\tau)e^{i\omega(t-\tau)}\,d\tau\,d\omega. \tag{6}$$

Note that any valid Fourier transform pair will produce the same result as in equation (6). The expression in equation (6) will be referred to as the general form of the system response function for a given input. Because $p(t)$ is defined to be nonzero only over a finite interval of time, equation (6) can be rewritten in the form

$$y(t) = \left(\frac{1}{2\pi}\right)\int_{-\infty}^{+\infty} H(\omega)\left(\int_{t_0}^{t_1} p(\tau)e^{i\omega(t-\tau)}d\tau\right)d\omega, \tag{7}$$

which makes explicit the finite time duration of the input pulse.

The form of equation (7) is a theoretical result on the use of steady-state system behavior to determine a response due to an arbitrary finite time duration pulse. In practice, the values on the right side of this equation are not available in a continuous form; they are only sampled values. Furthermore, in practice, only the real part of $y(t)$ is needed, and, in the remainder of this report, it is assumed that the system response is given by the real part of $y(t)$. When the transfer function is sampled at a discrete set of frequencies $\{\omega_j\}$, the frequency integral can be replaced by a summation to obtain

$$y(t) \approx \left(\frac{1}{2\pi}\right)\mathrm{Re}\left\{\sum_{\omega_j} H(\omega_j)\delta\omega\int_{t_0}^{t_1} p(\tau)e^{i\omega_j(t-\tau)}d\tau\right\}, \tag{8}$$

where $\delta\omega$ is the uniform spacing between frequency samples $\{\omega_j\}$. By further assuming that the input pulse is only available in the form of a sampled time series sampled at the discrete set of time points $\{t_k\}$, the system response function becomes

$$y(t) \approx \left(\frac{1}{2\pi(t_1 - t_0)}\right)\mathrm{Re}\left\{\sum_{\omega_j} H(\omega_j)\delta\omega\sum_{\tau_k} p(\tau_k)e^{i\omega_j(t-\tau_k)}\delta\tau\right\}, \tag{9}$$

where $\delta\tau$ is the uniform spacing between time samples. This expression is a discrete form of equation (7) that makes use of the finite time extent of the incident pulse $p(t)$. The necessary values of these spacings for an accurate solution, as well as the range of frequency samples required, are issues that are addressed using sampling theory, along with some basic knowledge of the system being modeled. It should be noted that fast Fourier transform techniques[4] can be used to represent the integral found in equation (8). Such techniques will improve overall computational efficiency, but do not affect the results of the comparative study of two techniques that are examined in this report.

The sampling theorem can be summarized as follows. A time signal whose spectrum (Fourier representation) has only zero components outside the finite frequency band from $f = f_1$ to $f = f_2$ can be uniquely determined by its values at (uniform) time samples spaced by

$$\Delta t = \frac{1}{2(f_2 - f_1)}. \tag{10}$$

The sampling interval given by equation (10) is referred to as the Nyquist sampling rate. This is only a theoretical result, since all real pulses (i.e., those with finite time extent) must have frequency components over an infinite frequency band. However, practice shows that, *for acoustics applications*, a band that encompasses those frequency components whose Fourier magnitudes are greater than one-tenth of the maximum spectral magnitude provides an acceptable frequency band. This limitation on the practical frequency domain of the input pulse provides the necessary time sampling of the pulse (via equation (10)) as well as the time sampling of the resulting output time series, which are sampled at the same rate. Another practical rule-of-thumb in the use of sampling to create digital pulses is to sample at twice the Nyquist rate, or at a $\Delta t$ that is one-half of what is given by equation (10).

A second issue that arises in the direct use of the sampling theorem is that the system must be basebanded to directly apply the sampling theorem to a frequency range that does not extend to zero. While basebanding may be a common practice in signal processing, it is difficult to perform in modeling since both the input pulse and the system impulse response must be basebanded in an identical manner in order to arrive at a result that can be transformed back to the proper frequency range. To avoid this problem, the system will be sampled assuming that the lower limit of the frequency range ($f_1$ in equation (10)) is equal to zero. This, along with the other practical sampling issues stated above, leads to a practical time sampling rule of

$$\Delta t = \frac{1}{4 f_2}, \tag{11a}$$

where

$$f_2 = \max\{f\} \ni \left\{ |F\{p(t)\}| \le \left( \frac{\max|F\{p(t)|}{10} \right) \right\}. \tag{11b}$$

Expression (11) may look complicated in mathematical notation, but it merely states that the sampling frequency is four times the maximum frequency of a frequency band given by the 20-dB down points of the power spectrum of the incident pulse.

The frequency limitations used in the development of the time sampling in equation (11) can also be used to develop a compatible limitation on the frequency band bounds for the transfer function $H(\omega)$. Define $f_1$ by

$$f_1 = \min(f) \ni \left\{ |F\{p(t)\}| \le \left( \frac{\max|F\{p(t)|}{10} \right) \right\}. \tag{12}$$

Now $f_1$ and $f_2$ define the bounds for the frequency band for the transfer function evaluation of the system response. The remaining parameter necessary for the evaluation of the system response function given in equation (9) is to determine the frequency step size to use in establishing the set $\{\omega_j\}$.

The step size to use in frequency stepping is an issue that is different for modeling purposes than it is in the signal processing community. The frequency step that is used affects the inverse Fourier transform (equation (5b)) by forcing a periodicity of the resulting time series. That is, if an inverse Fourier transform is made in a discrete manner with steps of $\delta\omega$, then the continuous inverse Fourier transform becomes the discrete inverse Fourier transform as follows:

$$g(t) = \frac{1}{2\pi}\int_{-\infty}^{+\infty} G(\omega)e^{i\omega t}\,d\omega \quad \Rightarrow \quad g(t) = \sum_{n=-\infty}^{+\infty} G(\omega_n)e^{i(n\delta\omega)t}\,. \tag{13}$$

From the above expression, it is easily seen that any time shift of the form $t \rightarrow t + T$, where $T$ is given by

$$T = m\left(\frac{2\pi}{\delta\omega}\right), \tag{14}$$

for any integer $m$, will not change the value of $g(t)$. Thus, any discrete inverse Fourier transform that is sampled at a frequency step of $\delta\omega$ will have, by necessity, a consequence of periodicity in time with a period of $T$ as given in equation (14). For the application of mathematical modeling of linear input/output systems as addressed in this report, this implies that the model result $y(t)$ will be periodic with a period $T$ as given in equation (14). Such a periodicity places a constraint on the maximal value to use for $\delta\omega$, which is simply

$$\delta\omega \leq \frac{2\pi}{T_0}, \tag{15}$$

where $T_0$ represents the minimum length of time for which there is output from the input/output process. This time extent must be obtained from the physics of the process being modeled, and is not purely a mathematically derived quantity for a process modeling problem. The practical limitation on this value for acoustic applications is what makes the direct method of Fourier realization impractical for many acoustic modeling tasks.

The number of points needed in time and frequency to properly construct an output time series can be quantified using the results to this point. Using equations (11) and (12), along with the input pulse, one can determine the frequency range and time step needed. Furthermore, the pulse length itself gives the extent of time needed to be modeled for only the input; the time extent of the output will, in general, be longer than that of the input for

transient system responses. Based on the output time extent, equation (15) can be used to set a frequency step. Thus, the number of frequency points $m$ required is given by

$$m = \left\lceil \frac{2\pi(f_2 - f_1)}{\delta\omega} \right\rceil \geq \lceil (f_2 - f_1) \cdot T_0 \rceil, \tag{16}$$

where $f_1$ and $f_2$ are as in equations (11) and (12). The notation $\lceil x \rceil$ is a common practice in mathematics literature used to represent the smallest integer greater than or equal to $x$. Similarly, the symbol $\lfloor x \rfloor$ represents the largest integer less than or equal to $x$. The number of time points required for the input $n_{in}$ and the output $n_{out}$ are given by

$$n_{in} = \left\lceil \frac{t_1 - t_0}{\Delta t} \right\rceil = \lceil 4 f_2 \cdot (t_1 - t_0) \rceil, \tag{17}$$

and

$$n_{out} = \left\lceil \frac{T_0}{\Delta t} \right\rceil = \lceil 4 f_2 T_0 \rceil. \tag{18}$$

Therefore, the double sum in equation (9) must be taken at $m$ frequency points and $n_{in}$ time points for a total of $M$ time-frequency points, where

$$M = m \cdot n_{in} = \lceil 4 T_0 f_2 (f_2 - f_1)(t_1 - t_0) \rceil. \tag{19}$$

Each of these $M$ time-frequency points are used in the evaluation of output at each of the $n_{out}$ output time steps. From expression (19), it is obvious that $M$ is large when the input signal has a large time-bandwidth product and/or when the output time extent required is very long. When both of these conditions occur, the problem becomes computationally very costly.

## TRANSIENT PULSE RESPONSE MODELING FOR MULTIPLE SUBSYSTEMS

When a system is composed of multiple independent subsystems, the practical application of transient pulse response modeling becomes computationally costly. This problem arises frequently in acoustic modeling, such as propagation modeling using a summation of acoustic eigenrays, or acoustic scattering from a structure composed of multiple independent highlights. In these cases, steady-state models of the individual subsystems have been created because of computational and/or theoretical simplicity. Due to the linearity of acoustics, the results of these subsystems may be combined using linear superposition to arrive at a single steady-state result for the composite system. In this section, the extension of the single system case to multiple subsystems is explained, and an efficient computational method for handling the multiple subsystem case is derived.

Assume that a system with transfer function $H(\omega)$ is composed of $N$ independent subsystems, with linear transfer functions $\{H_n(\omega)\}$ such that

$$H(\omega) = \sum_{n=1}^{N} H_n(\omega). \tag{20}$$

This kind of separation into subsystems is often done when steady-state models (analytical and/or computational) of the individual subsystems are readily available. However, in order to apply equation (20) to a physical modeling problem, a number of conditions must be met. First, each of the subsystems must be a linear, time-invariant system. The time-invariance implies that an input of $u(t + t_d)$, for any time delay $t_d$, will produce the output $y(t + t_d)$. Note that this type of time-invariance will maintain any relative time delays between different subsystems, since the delay is applied to the input, not the system impulse response function. Secondly, the subsystems must be linearly independent from one another to allow the superposition principle to hold. Finally, each of the subsystems must be causal, i.e., there can be no dependence on any past input or state for any of the given subsystems. Thus, the response to any of the given subsystems does not depend on any of the other subsystems.

The standard approach to modeling a multiple subsystems problem is to use equation (20) directly by summing the component transfer functions in the frequency domain and using that result as the composite system transfer function. This result is accurate, but may be extremely computationally costly. Consider the following simple example. A system of $N$ subsystems has transfer functions that are given by

$$H_n(\omega) = A_n e^{i\omega\xi_n}, \tag{21}$$

for positive $A_n$ and $\xi_n$. The time-domain output of the composite system is given by

$$y(t) = \sum_{n=1}^{N} A_n u(t + \xi_n), \tag{22}$$

which is a sequence of scaled and time-shifted replicas of the input pulse. If the input pulse has a time extent that is nonzero over a range from $t_0$ to $t_1$, then the resulting necessary time extent of the output will be given by

$$T_0 = (\max\{\xi_n\} - \min\{\xi_n\}) + (t_1 - t_0). \tag{23}$$

This number directly affects the number of frequency samples needed for accurate pulse output modeling as shown by equation (16). The form of the expression in equation (23) shows that the number of frequency samples required can (in this particular case) scale linearly with the difference in time delays between subsystems.

The result of this simple example shows that the number of frequency samples required can become very large when the relative time delays between subsystems become large. In this example, the number of frequency samples required for the output representation is found from equation (16) to be

$$m = (f_2 - f_1)(t_1 - t_0) + (f_2 - f_1)(\max\{\xi_n\} - \min\{\xi_n\}). \tag{24}$$

The first term in this expression is equal to the number of frequencies required to model the input pulse in a Fourier representation, which is added to a term that accounts for the different time delays found in the various subsystems. Most signal processing applications only window a time series over the length of the input pulse; therefore, in that case, the second term in this expression is negligible. However, in the mathematical modeling of pulse responses, both terms in equation (24) are required for a satisfactory solution. This use of the direct summation of subsystem transfer functions for modeling will be referred to as the direct approach for the remainder of this report.

In the general setting, consider a system comprised of $N$ subsystems with transfer functions $\{H_n(\omega)\}$. Each of the subsystem responses can be placed in the form of a secondary transfer function $H_n(\omega)$ and a time delay of $\xi_n$, such that the subsystem transfer function is

$$H_n(\omega) = \hat{H}_n(\omega) e^{i\omega\xi_n}, \tag{25}$$

where the secondary transfer function contains no additional time delays. That is, if the input pulse begins at time $t = 0$, then the secondary transfer function has an output that also begins at time $t = 0$. In this way, the time delay feature of the subsystem transfer function has been separated from the remaining effects of the subsystem transfer function.

Once all of the subsystem transfer functions have been properly separated as shown in equation (25), the result of the total system output can be derived from equation (9) as

$$y(t) \approx \left( \frac{1}{2\pi(t_1 - t_0)} \right) \sum_{n=1}^{N} \mathrm{Re}\left\{ \sum_{\omega_j} \hat{H}_n(\omega_j) e^{i\omega_j (t+\xi_n)} \delta\omega \sum_{\tau_k} p(\tau_k) e^{-i\omega_j \tau_k} \delta\tau \right\}. \tag{26}$$

This expression is even more computationally intensive than the transfer function summation method (the direct approach); however, equation (26) is greatly simplified under a constraint. If the subsystem time-delays $\xi_n$ are all constrained to lie on steps of the output time axis $t$, then the exponential expression in the middle of equation (26) is just a discrete time shift of the axis of the form

$$t \mapsto t + \xi_n, \tag{27}$$

for each of the $N$ subsystems. Note that if the added constraint were not made, the evaluation of equation (26) along a discrete time axis would be impractical, since each subsystem would, in general, be on a slightly shifted time axis. With the added constraint, the final form can be written as

$$y(t) \approx \sum_{n=1}^{N} \mathrm{Re}\{\hat{y}_n(t + \xi_n)\}, \tag{28}$$

where

$$\hat{y}_n(t) = \left( \frac{1}{2\pi} \right) \sum_{\omega_j} \hat{H}_n(\omega_j) P(\omega_j) e^{i\omega_j t} \delta\omega, \tag{29}$$

and $P(\omega_j)$ is the discrete form of the Fourier transform (as in equation (5)) of $p(t)$ evaluated at a frequency of $\omega_j$. The use of equations (25), (28), and (29) combined creates a computationally efficient method of representing the combination of multiple subsystem responses.

In practice, the assumption that all of the subsystem delays (as shown in equation (25)) lie exactly on the discrete steps of the output time axis is impractical. In that case, the subsystem transfer function is first placed in a form similar to equation (25), which is given by

$$H_n(\omega) = \tilde{H}_n(\omega) e^{i\omega(\xi_n + \zeta_n)}, \tag{30}$$

where the total time delay of the subsystem is $\Delta t_n = (\xi_n + \zeta_n)$. Since the model output for each subsystem will contain the total time delay, the parameters $\xi_n$ and $\zeta_n$ are somewhat arbitrary. Any combination whose sum equals the total subsystem time delay will be accurate, but computational efficiency is met when they are chosen such that

$$\xi_n = \left\lfloor \frac{\Delta t_n}{t_{step}} \right\rfloor \cdot t_{step} \qquad \text{and} \qquad \zeta_n = \Delta t_n - \xi_n, \tag{31}$$

where $t_{step}$ is the uniform spacing of samples in the output time axis. Now the transfer function representation for the subsystem is given as shown in equation (25) with

$$\hat{H}_n(\omega) = \tilde{H}_n(\omega) e^{i\omega\zeta_n}. \tag{32}$$

In this manner, the transfer functions of each of the subsystems have been accurately shifted so that the subsystem time delays all line up with the time steps on the output time axis. By performing this transformation for the slight shifting along the time axis, the interference effects (both constructive and destructive) that occur due to multiple subsystems overlapping in time are maintained exactly. The outputs from the subsystems can then be added together coherently on the output time axis to obtain the same result (up to round-off error) that would be obtained using a single transfer function as in equation (20). The use of equation (31) eliminates any errors due to slight shifting of the subsystems along the time axis to line up with the time steps.

The computational requirements of a system modeled using the efficient technique can be addressed in the same manner as for the direct approach. Let $T_n$ denote the time extent of each of the output pulses for the subsystems. In the case of an input pulse that exists from $t = t_0$ to $t = t_1$, the output pulse for the $n^{th}$ subsystem exists (is nonzero) over the time interval from $t = (t_0 + \xi_n)$ to $t = (t_0 + \xi_n) + T_n$. From equation (29), it is seen that the output pulses for each subsystem will be computed independently; thus all of the $T_n$ values are independent. Each of the subsystems has its own frequency summation in equation (29); therefore, using equation (16), the number of frequency samples that must be computed for each subsystem is

$$m_n = \lceil (f_2 - f_1) \cdot T_n \rceil. \tag{33}$$

It must be remembered that the number of frequency samples required is also the number of times that the steady-state model must be exercised to obtain the transfer function samples $\{H_n(\omega_j)\}$. In the case of the efficient technique, each subsystem only is run at $m_n$ frequencies (as shown in equation (33)), while the direct approach requires all subsystems to be computed at the $m$ frequency samples as given by equation (16). Assuming that all subsystems require the same amount of computational effort per frequency, and representing the effort for computing the transfer function of an individual subsystem at an individual frequency by $E_0$, the total computational effort in frequency computations for the two techniques is

$$E_D = \sum_{n=1}^{N} m E_0 = (N E_0) \cdot \lceil (f_2 - f_1) \cdot T_0 \rceil, \tag{34}$$

for the direct approach, and

$$E_E = \sum_{n=1}^{N} m_n E_0 = \sum_{n=1}^{N} E_0 \lceil (f_2 - f_1) \cdot T_n \rceil, \tag{35}$$

for the efficient technique. The number of time points for the input ($n_{in}$ as in equation (17)) is the same for both techniques. The number of time points for the output for the direct approach is given by equation (18), and for the efficient technique is given by the same expression with $T_0$ replaced by a summation over all of $\{T_n\}$. Since the Fourier convolution computations are, in general, not as costly computationally as the running of the steady-state model, they have little impact on overall computational effectiveness. (The relative costs of the convolutions used in the two techniques will be discussed.)

From the computational requirements shown in equations (34) and (35), it is clear that the efficient technique is appropriately named in most cases. In fact, the difference in computational effort between the two techniques can be written as

$$\begin{aligned} \Delta E &= E_E - E_D \\ &= E_0 \cdot \left\lceil \left( \sum_{n=1}^{N} T_n - N T_0 \right) (f_2 - f_1) \right\rceil \le 0, \end{aligned} \tag{36}$$

with equality holding only when $T_n = T_0$ for all $n$. This expression shows the improvement in using the computionally efficient technique over the direct approach for all cases of practical interest. Furthermore, the *a priori* determination of the subsystem $T_n$'s (or an upper bound on them) is usually much more easily obtained than an *a priori* estimate on the upper bound of $T_0$. Thus, in practice, the value of $T_0$ that must be used is very large compared to the true value, which can only be obtained from the resulting output. This observation will become evident in the examples found in the following sections.

There is an added cost for the efficient technique in that Fourier convolutions of the form of equation (29) must be performed for each subsystem. However, the Fourier evaluation of the incident pulse $p(t)$ only needs to be performed once, since all subsystems use the same frequency spacings. Using a straightforward inverse Fourier transform technique for the convolutions requires

$$m_n \cdot (2m_n)^2 = O(m_n{}^3) \tag{37}$$

complex multiplication operations for each subsystem (other simple operations, such as addition, are not included due to their relative efficiency). If an inverse fast Fourier transform technique[4] is employed, the number of complex multiplications is

$$m_n \cdot O(m_n \log_2 m_n) = O(m_n{}^2 \log_2 m_n). \tag{38}$$

The expressions in equations (37) and (38) give the number of multiplications required to create the interpolates for Fourier series that are evaluated at each time point to arrive at pulse responses in the time domain. The direct technique has similar expressions, but is only performed once for the composite system, not separately for each of the $N$ subsystems. If $F_D$ and $F_E$ represent the computational cost of performing the required Fourier convolutions for the two techniques, the computational difference in the convolution evaluations can be written as

$$\Delta F = F_E - F_D$$

$$= O(N \cdot m_n \log_2 m_n) - O(m \log_2 m). \tag{39}$$

This number is close to zero in most applications and can therefore be disregarded in many cases. However, when there are many subsystems and the number of frequencies used in the efficient technique is not appreciably lower than the direct technique, then the computational cost of the Fourier convolutions should be taken into consideration.

The standard technique for transient pulse response modeling for multiple subsystems is transfer function addition. This technique is summarized by equations (9) and (20). The efficient technique that has been developed is shown by equations (25), (28), (29), and (32), and has been shown to require far fewer runs of the steady-state models to maintain the same degree of accuracy. The computational effort analysis that was performed assumes the majority of the computational effort involved in this process is in running a steady-state model at a number of frequencies for each of the subsystems (transfer function evaluation). The main improvement in the efficient technique is in the reduction in the number of frequencies that are required. Two examples from acoustics (highlight-based acoustic scattering and ray-based acoustic propagation) will be shown to illustrate the performance improvement of the efficient technique.

## ACOUSTIC SCATTERING MODELING EXAMPLE

An example of a modeling task that can make use of the technique developed in this report is the modeling of high-frequency acoustic scattering using multiple highlight target models. In these applications, the acoustic scattering from a structure is represented as a composition of acoustic scattering from a number of discrete features (or highlights) that comprise the target. These individual highlight responses can then be linearly superimposed to create the composite echo return from the structure. Such techniques are common in high-frequency scattering where theories such as the Geometric Theory of Diffraction are applicable. In these cases, there is a natural division of the structure into a finite number of dominant highlights (or subsystems) whose linear superposition of responses well approximates the total response. The main goal of this example was to show the utility of using an efficient multiple response convolution algorithm as opposed to a direct technique. In that sense, it is assumed that the direct solution is correct, that this example is sufficiently representative of the general acoustic scattering modeling problem, and that the results drawn from it may be extended to other cases.

For the example in this report, a sample target comprised of 15 highlights was created. This target was modeled in a steady-state manner using the high-frequency target acoustic model (HFTAM) to obtain the complex monostatic response at a variety of frequencies for a fixed geometry. The HFTAM target model is used in high-frequency acoustic scattering modeling applications to predict the response (echo return) from a submarine structure that is actively ensonified. Previous applications of HFTAM used a narrowband approximation and modeled the pulse response as the center frequency response only. This application allows for the computation of echo returns from broadband pulses. Two geometries were used in this study, one at bow aspect and the other at near-beam aspect (80 degrees off-bow). In the near-beam aspect case, all of the highlights will return echoes at close to the same time, creating a large opportunity for coherent addition. In the bow aspect case, most of the highlights return echoes at very different times, creating very little opportunity for coherent addition. The study results will show that the efficient computational technique performs well in both situations.

For this example, the pulse that was chosen is a linear frequency modulator (LFM) pulse from 22 kHz to 25 kHz that was 4 msec in duration. The time-bandwidth product (TBP) of such a pulse is 12, which is broadband. The TBP is important in determining the need to represent a pulse with nonzero bandwidth (broadband) or by its center frequency alone (narrowband). If a pulse has a large bandwidth but a very short time duration, there are not enough cycles of energy at the different frequencies to make a broadband representation necessary. Most experts agree that any pulse with a TBP greater than 7 is a broadband pulse and should be modeled as such. Thus, the pulse in this study is definitely a broadband pulse and should be modeled with all of the necessary component frequencies. Note that the bandwidth used in computing the TBP is not the same as the frequency range used in the previous section to determine frequency spacing, which will always be larger.

For the efficient technique, the time extent for each of the subsystem responses was chosen to be $T_n$ = 8 msec (twice the input pulse length), and the 20-dB down-point frequencies used in the modeling were 20 kHz and 27 kHz. Based on these numbers, the frequency spacing necessary for pulse response modeling is 125 Hz; there are, therefore, 57 frequencies at which the subsystem steady-state responses (transfer functions) must be computed. For the direct technique, the time length $T_0$ could only be chosen *a priori* to be equal to twice the acoustic length of the target plus the pulse length, or 141 msec (the nominal target length of this generic structure is 100 m). This is a definite drawback of the direct technique, where time extent is often chosen to be greater than necessary when the results of the model output are not available ahead of time. In this case, the direct technique required a frequency spacing of 7 Hz; there were, therefore, 1000 frequencies at which the subsystem steady-state responses were computed. This is a 17.9:1 difference in the number of target model runs that must be computed for the two techniques. Based on these results, the difference in the number of complex multiplications used in the Fourier convolution for the two techniques can be shown (see equation (39)) to be

$$\begin{aligned} \Delta F &= F_E - F_D \\ &= O(4878) - O(9966) \approx 0. \end{aligned} \tag{40}$$

It can be seen from this assessment that the computational improvement of transfer function generation for the subsystems (57 versus 1000 frequencies) of the efficient technique is quite dramatic and presents a major savings in run-time. The computational loads for Fourier convolution for the two different techniques are of the same order of magnitude and are considered unimportant in a comparative analysis.

The results of modeling the near-beam (80 degrees off-bow) scattered response of this pulse using HFTAM and the two pulse response techniques are shown in figure 1. From this time series representation, it is clear that the two pulses are nearly indistinguishable. The many additional frequencies of the direct technique were needed so that the summation of Fourier modes provides the zero solution (seen from 0 to 60 msec and 80 to 150 msec in figure 1). Since the efficient technique only computes a solution where it is expected to be nonzero, there are much fewer Fourier modes required (much less cancellation of modes to create a zero solution for a length of time). A good measure of the matching of the two techniques is to compute the spectrum of each pulse response over a region of time. An accurate match in both time and frequency domains will guarantee that most signal processing algorithms cannot distinguish between the two returns. For this case, a time region encompassing a majority of the returned energy (60 to 90 msec) was chosen. Figure 2 shows a plot of these spectra as well as the spectrum of the incident pulse. The spectra of the two pulse returns show that the direct and efficient techniques provide nearly identical solutions in the region of highest energy concentration. The efficient technique has a stronger trailing tail off of the main spectrum, caused by the sharp cutoff to zero in a finite time interval, whereas the direct technique will always have an exponential decay to zero. Furthermore, note that the spectra of the returns have a different shape than that of the incident pulse. This is an effect of both the broadband nature of the individual subsystem returns as well as the coherent addition of multiple subsystems.

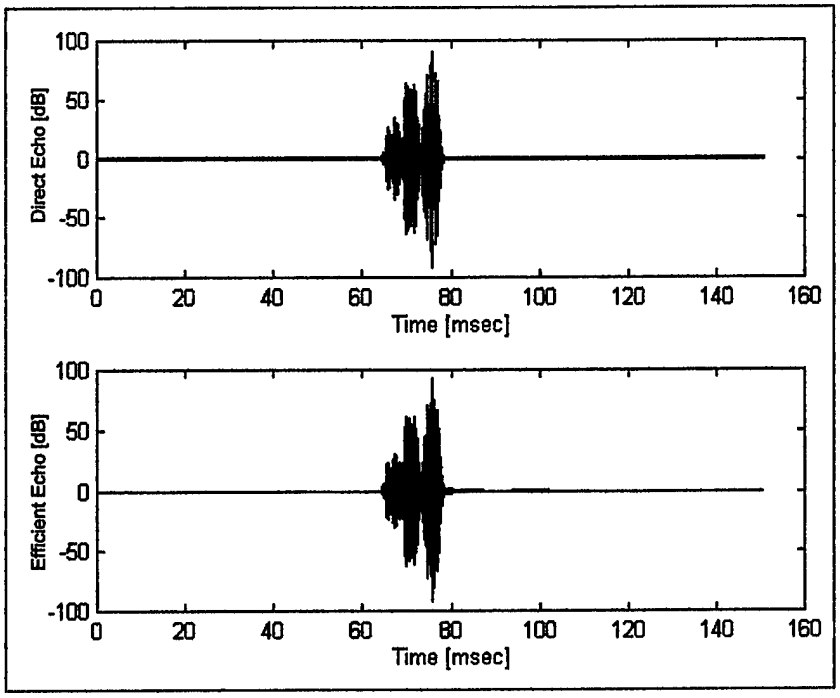


***Figure 1. Comparison of Direct and Efficient Echoes for Scattering Near-Beam Aspect***

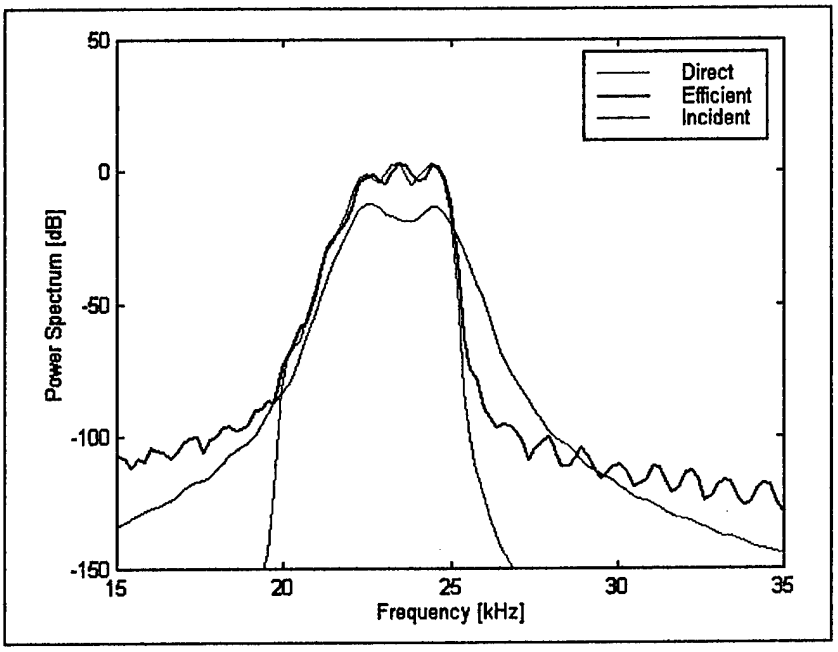


***Figure 2. Spectrum of the Echoes for Scattering Near-Beam Aspect for a Window from 60 to 90 msec***

The results of modeling the bow aspect scattered response of the same incident pulse using HFTAM and the two pulse response techniques is shown in figure 3. Once again, the time response of the result using the two techniques appear to be nearly identical. As in the case of the near-beam response, the best comparison of the two results is made by looking at the frequency domain response. Since there are distinct regions of time where the energy of the return is concentrated, multiple spectra will be computed for each of these regions of time.

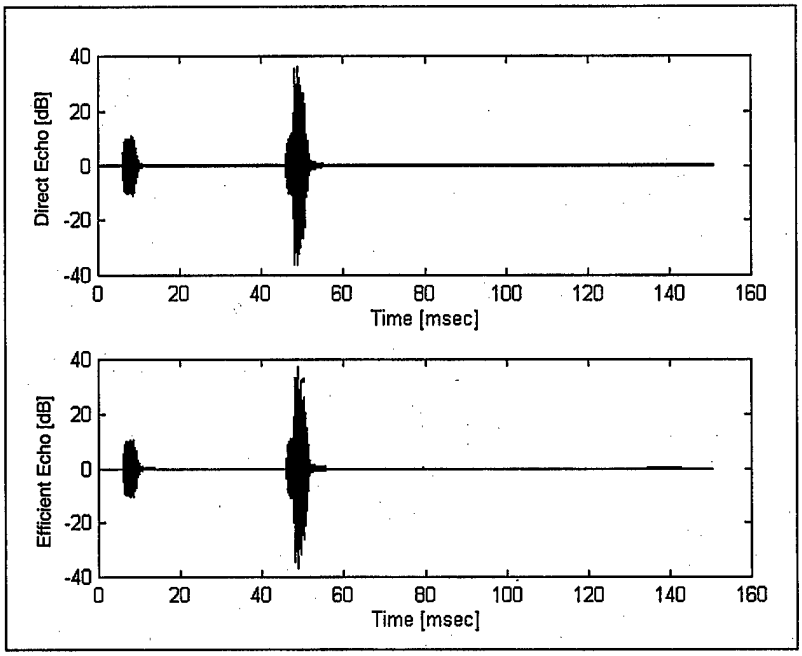


***Figure 3. Comparison of Direct and Efficient Echoes for Scattering at Bow Aspect***

Figures 4 and 5 show two of the regions of time, from 0 to 20 msec and from 40 to 60 msec, respectively. The first of these regions (shown in figure 4) contains the response from only a single highlight, and the match between techniques is nearly identical. However, it should be pointed out that even in this single highlight case, the spectral shape of the return is different than that of the incident pulse. This is the primary feature of broadband pulse response models. Also, the tail of the spectrum for the efficient technique is larger than that of the direct technique. As before, this is a consequence of the finite time duration of the efficient technique's response. The spectra in figure 5 contain the returns from multiple highlights that are superimposed over each other in time. The spectra match very closely and contain a combination of multiple highlight features (superposition) as well as broadband characteristics of each of the highlights. The region of time beyond the primary energy does have some small amplitude highlight responses, and their spectra are shown in figure 6. It can be seen that the two techniques vary slightly in their responses; however, this is because the direct technique has some of the exponential time decay of the larger amplitude returns corrupting these very small amplitude returns. Since this is only

an effect on the very smallest of returns (relatively small within any given pulse return), it is not a problem for the overall echo response. Thus, the efficient technique matches the direct technique result very well at a greatly reduced computational cost.

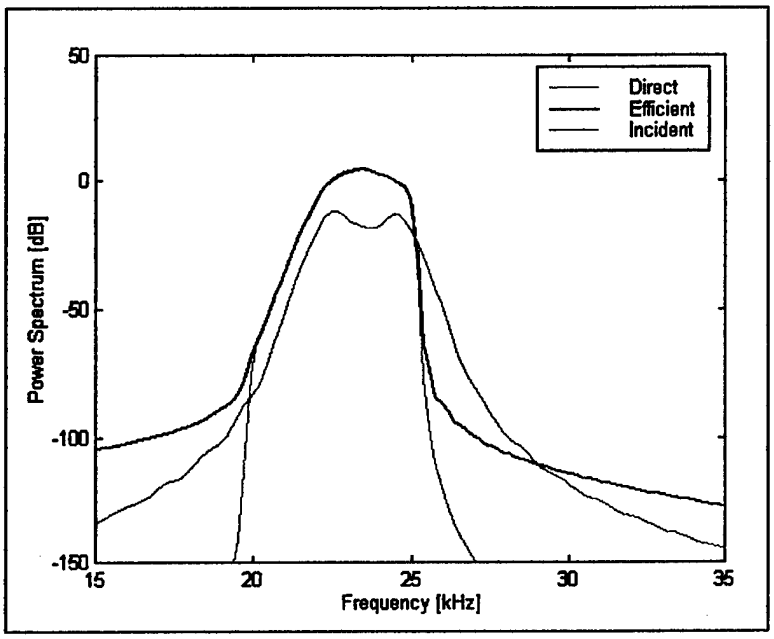


***Figure 4. Spectrum of the Echoes for Scattering at Bow Aspect with a Window from 0 to 20 msec***

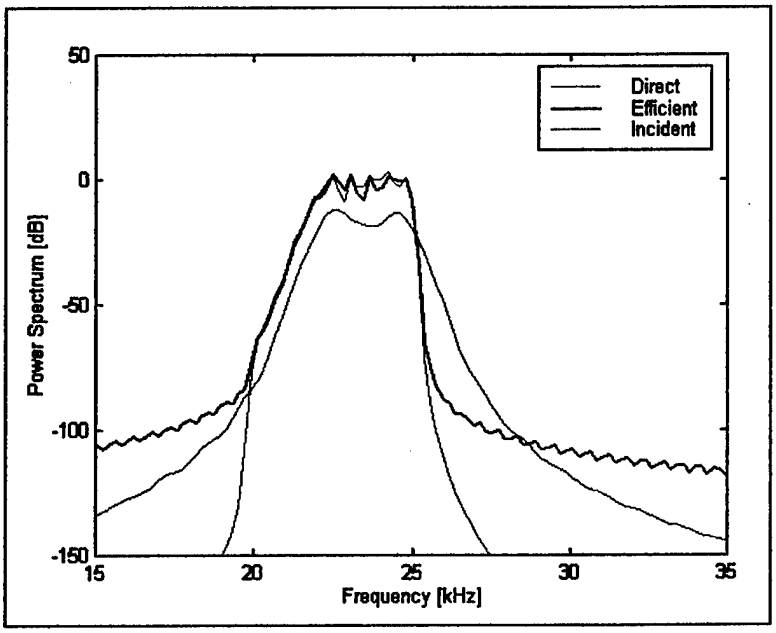


***Figure 5. Spectrum of the Echoes for Scattering at Bow Aspect with a Window from 40 to 60 msec***

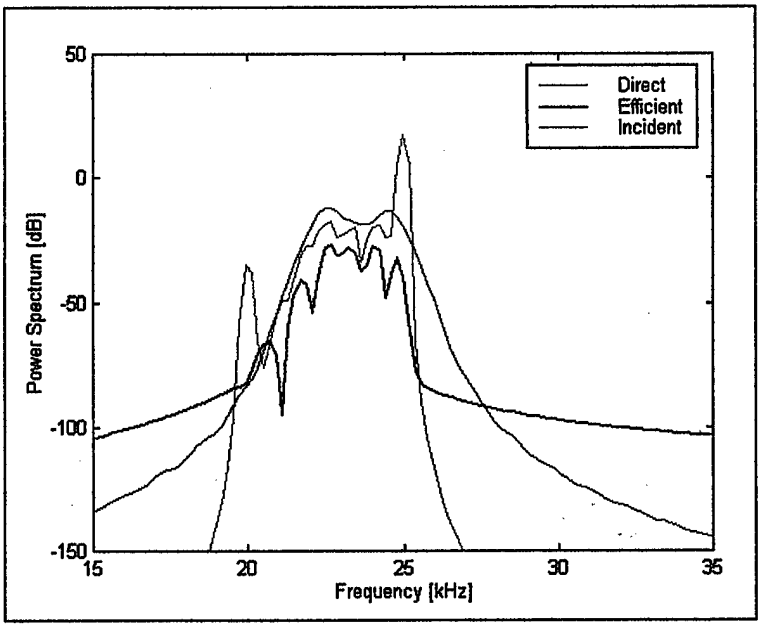


***Figure 6. Spectrum of the Echoes for Scattering at Bow Aspect with a Window from 60 to 150 msec***

## ACOUSTIC PROPAGATION MODELING EXAMPLE

For the case of acoustic propagation modeling, the Naval Undersea Warfare Center's comprehensive acoustic system simulation (CASS) model was used in conjunction with the Gaussian ray acoustic bundling (GRAB) propagation model[5] along with Navy standard bottom and surface bounce models. This combination of models has been proven to be effective in modeling acoustic reverberation data. The main goal of this study, as that of the scattering example, was to show the utility of using an efficient multiple response convolution algorithm as opposed to a direct technique. In that sense, it was assumed that the direct solution is correct, and that this example is sufficiently representative of the general acoustic propagation modeling problem that results drawn from it may be extended to other cases.

The runs that were made all used a range of 2 kyd and the same incident pulse as used in the acoustic scattering example (a 4-msec LFM from 22 to 25 kHz). The environmental model performs a ray trace[6] for a sequence of test rays, spaced every 0.25 degrees in the vertical aperture. The CASS model (with GRAB propagation sub-models) computes a Gauss-weighted averaging of these rays into a set of eigenrays, whose combined pressure levels mimic the true pressure. In the context of this report, the division of the acoustic propagation problem into eigenrays is the subsystem breakdown that will be used in the efficient computational technique.

For the efficient technique, the time extent for each of the subsystem responses was chosen to be $T_n$ = 8 msec (twice the input pulse length), and the 20-dB down-point frequencies used in the modeling were 20 kHz and 27 kHz. Based on these numbers, the frequency spacing necessary for pulse response modeling is 125 Hz; there are, therefore, 57 frequencies at which the subsystem steady-state responses (transfer functions) must be computed. There were also nine eigenrays arriving at the range of interest, and, thus, nine subsystems. For the direct technique, the time length $T_0$ could only be chosen after running the model once at a nominal frequency, the center frequency of 23.5 kHz in this case, and comparing the relative time delays of the eigenrays. The difference between the maximum and minimum eigenray delay times was 54 msec; adding double the pulse length to this makes $T_0$ = 62 msec. The requirement to make a single frequency run of the environmental model before choosing $T_0$ is a distinct drawback to the direct technique. Based on this analysis, the direct technique required a frequency spacing of 16 Hz, and there were, therefore, 438 frequencies at which the subsystem steady-state responses were computed. This is a 7.7:1 difference in the number of target model runs that must be computed for the two techniques. Based on these results, the difference in the number of complex multiplications used in the Fourier convolution for the two techniques can be shown (see equation (39)) to be

$$\begin{aligned}\Delta F &= F_E - F_D \\ &= O(2992) - O(3843) \approx 0.\end{aligned} \tag{41}$$

It can be seen from this assessment that the computational improvement of transfer function generation for the subsystems (57 versus 438 frequencies) of the efficient technique is dramatic (although not as much as in the scattering example) and presents a major savings in runtime. The computational loads for Fourier convolution for the two different techniques are of the same order of magnitude and are considered unimportant in a comparative analysis.

The results of modeling the propagation of the broadband pulse with the two techniques are shown in figure 7. From this time series representation, it is clear that the two pulses are nearly indistinguishable. The many additional frequencies of the direct technique were needed so that the summation of Fourier modes provides the zero solution. Since the efficient technique only computes a solution where it is expected to be nonzero, there are much fewer Fourier modes required (much less cancellation of modes to creates a zero solution for a length of time). To compare the two time series, the spectrum of each pulse response over a region of time is again computed. An accurate match in both time and frequency domains will guarantee most signal processing algorithms cannot distinguish between the two returns. For this case, two time regions were examined. The first time region, from 5 to 13 msec, had multiple eigenrays arriving at time delays that caused the output pulses to overlap. (Its spectra is shown in figure 8.) Both the efficient and direct techniques have nearly identical spectra near the peak, and their spectra are different from the incident pulse, thus, showing an effect of the superposition of multiple eigenrays. The second time region examined is from 32 to 40 msec, where only a single eigenray returned with a time delay in that region. These spectra are shown in figure 9 and again match each other very well. In this case, the spectra are similar in shape (although

not magnitude) to the incident spectrum, an effect of the single eigenray. For both of these cases, as in the scattering examples, the efficient technique has a stronger trailing tail off of the main spectrum, caused by the sharp cutoff to zero in a finite time interval, whereas the direct technique will always have an exponential decay to zero.

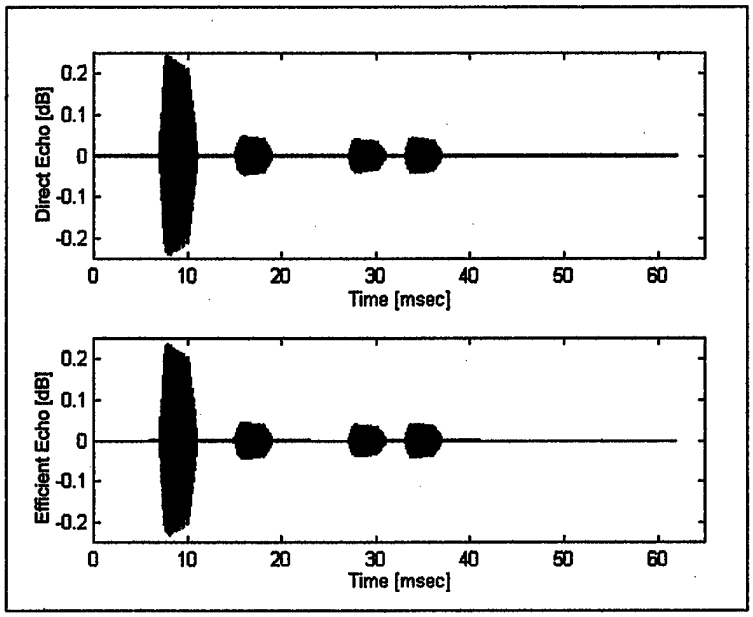


***Figure 7. Comparison of Direct and Efficient Echoes for Propagation at a Range of 2 kyd***

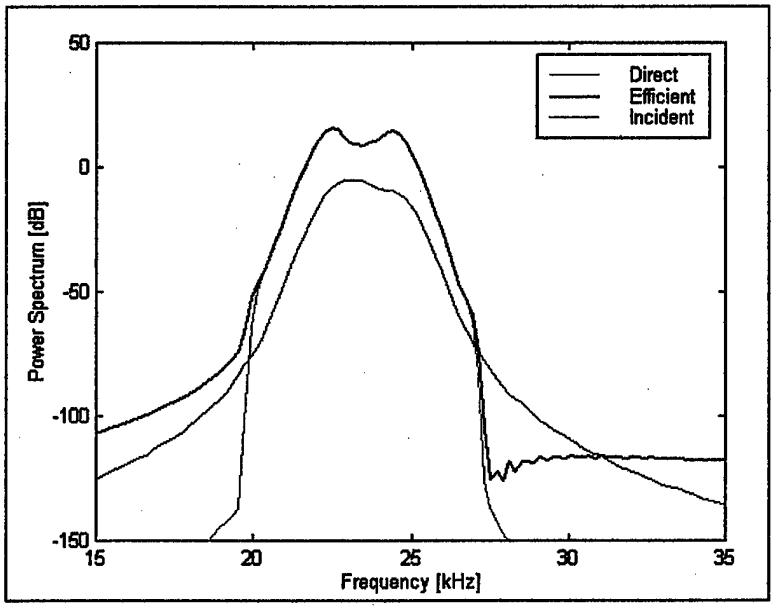


***Figure 8. Spectrum of the Pulses for 2-kyd Propagation with a Window from 5 to 13 msec***

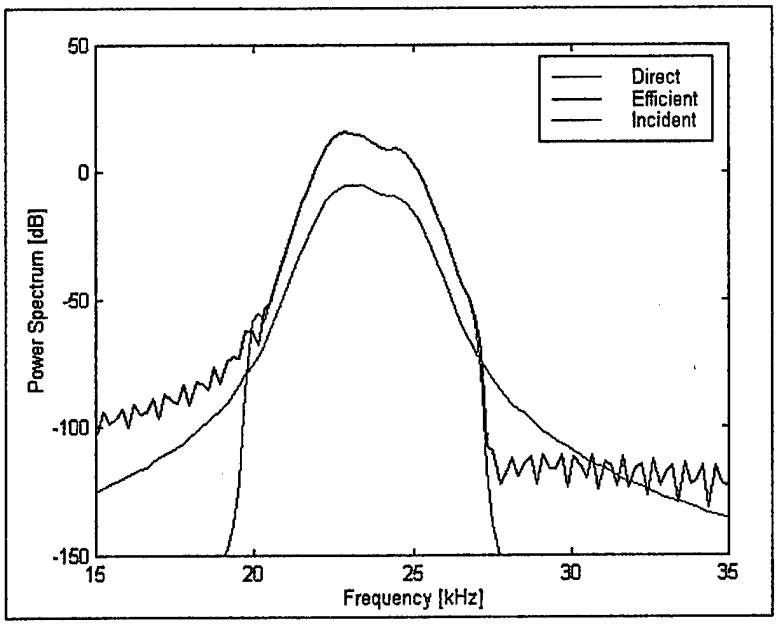


***Figure 9. Spectrum of the Pulses for 2-kyd Propagation with a Window from 32 To 40 msec***

## CONCLUSIONS

This report has presented two techniques for convolving a time domain pulse with model-generated transfer functions of systems composed of multiple subsystems. The first technique was a direct method whereby the individual subsystem transfer functions were summed and the resulting total system transfer function was convolved with the pulse. An alternative technique of convolving individual subsystems with the pulse and adding the results together in the (discretized) time domain was also presented. Details of the computational implementation of the technique, including frequency step, frequency range, time step, etc., were derived from standard modeling and processing principles.

An analysis of the computational requirements of the two techniques showed that the subsystem technique provided a more efficient calculation almost all of the time; thus, it was referred to as the "efficient" technique. The two main components of any of these model-based convolution techniques are running the model a number of times to generate the transfer function, and performing the numerical Fourier convolution. It was shown that the efficient technique always requires less effort for the former, and the effort of the latter is almost always lower for the efficient technique (the exception is when there are many subsystems that all contain approximately the same time delay). Furthermore, the efficient technique was shown to require less *a priori* information than the direct technique, and, thus, is more suited to a completely automated modeling framework.

The two techniques were each applied to two examples of Navy interest: acoustic scattering from a submerged structure and acoustic propagation in the ocean medium. Both cases illustrated that the efficient technique can significantly improve computational speed while maintaining accuracy. Analysis of both time and frequency domain descriptions of the output from the two techniques showed the results to be virtually indistinguishable between the two techniques, a conclusion that held for both areas of application.

The results of this report identify a computationally efficient technique for convolution of signals with linear systems composed of multiple linear subsystems. Two examples of Navy application showed the effectiveness and utility of the technique. It is recommended that this efficient technique be applied to model-based convolution whenever there are multiple subsystems being modeled. The technique will be especially important in broadband pulse convolution with models in a simulation setting.

## REFERENCES


1. J. S. Bendat and A. G. Piersol, *Engineering Applications of Correlation and Spectral Analysis*, John Wiley and Sons, Inc., New York, 1980.

2. T. Kailath, *Linear Systems*, Prentice-Hall, Englewood Cliffs, NJ, 1980.

3. A. V. Oppenheim, A. S. Willsky, and I. T. Young, *Signals and Systems*, Prentice-Hall, Englewood Cliffs, NJ, 1983.

4. D. F. Elliott and K. R. Rao, *Fast Transforms: Algorithms, Analyses, Applications*, Academic Press, New York, 1982.

5. H. Weinberg and R. E. Keenan, "Gaussian Ray Bundles for Modeling High-Frequency Propagation Loss Under Shallow Water Conditions," NUWC-NPT Technical Report 10,568, Naval Undersea Warfare Center Division, Newport, RI, April 1996 (UNCLASSIFIED).

6. C. S. Clay and H. Medwin, *Acoustical Oceanography: Principles and Applications*, John Wiley and Sons, Inc., New York, 1977.

## INITIAL DISTRIBUTION LIST

| Addressee | No. of Copies |
|---|---|
| Space and Naval Warfare Systems Center, San Diego (D. Dickerson) | 1 |
| Office of Naval Research (ONR 333, K. Latt) | 1 |
| Applied Research Laboratory, Pennsylvania State University (F. R. Menotti, R. L. Culver) | 2 |
| Defense Technical Information Center | 2 |